Rare-Earth Solid-State NMR Spectroscopy of Intermetallic Compounds: The Case of the ^{175}Lu Isotope

Christopher Benndorf[a, b], Marcos de Oliveira Junior[c], Henrik Bradtmüller[d], Frank Stegemann[a], Rainer Pöttgen[a], and Hellmut Eckert[c, d]*

[a] Institut für Anorganische und Analytische Chemie, Westfälische Wilhelms-Universität Münster, Corrensstraße 30, 48149 Münster, Germany
[b] Institut für Mineralogie, Kristallographie und Materialwissenschaft, Universität Leipzig, Scharnhorststraße 20, 04275 Leipzig, Germany
[c] Instituto de Física de São Carlos, Universidade de São Paulo, CEP 369, São Carlos, SP 13566-590, Brazil
[d] Institut für Physikalische Chemie, WWU Münster, Corrensstraße 30, 48149 Münster, Germany, E-Mail: eckerth@uni-muenster.de

Abstract

The feasibility of high-resolution ^{175}Lu solid-state NMR spectroscopy in intermetallic compounds crystallizing with cubic crystal structures is explored by magic-angle spinning NMR at different magnetic flux densities. The large quadrupole moment of this isotope (3.49 $\times 10^{-28}$ m^2) restricts observation of the NMR signal to nearly perfectly ordered crystalline samples. Signals are successfully detected and analyzed in the binary pnictides Lu*Pn* (NaCl-type structure; *Pn* = P, As, Sb) and the intermetallic compounds LuPtSb and LuAuSn, both crystallizing with the MgAgAs-type structure. Sources of line broadening are discussed based on field-dependent static and MAS-NMR spectra, providing guidance with respect to measurement conditions resulting in reliable results. The results highlight the importance of ionic/covalent bonding effects for the detectability of the signal, which reduce the probability of real structure effects commonly observed in intermetallic compounds. No ^{175}Lu NMR signals can be observed in various cubic Heusler compounds. This is attributed to mixed site occupancies and other structural defects producing electric field gradients whose interaction with the ^{175}Lu quadrupole moments broadens the signal beyond detection.

1. Introduction

High-resolution solid-state NMR spectroscopy is a powerful probe for structural investigations of intermetallic compounds [1-4]. The excellent ability of NMR spectroscopy to differentiate between atoms on crystallographically inequivalent sites in a quantitative fashion makes this method very useful to confirm proposed crystal structure models from X-ray diffraction by comparison of signal intensities with predicted site multiplicities. The quality and validity of a proposed crystal structure can be tested further by comparing the nuclear electric quadrupolar coupling constants and asymmetry parameters computed directly from crystal structure data with those measured from NMR spectroscopy. Such structure validation by NMR spectroscopy becomes especially important for compounds based on elements with nearly similar scattering power, for materials presenting single crystals of low quality or twinning, and for those cases where only polycrystalline or amorphous samples are available. Finally, the ability of NMR spectroscopy to resolve locally distinct environments allows in-depth characterization of order/disorder phenomena including: 1) occupancy deficiencies in non-stoichiometric compounds, 2) site multiplicities produced by positional disordering, and 3) superstructure formation, polymorphism and phase transitions. In metallic compounds, the resonance frequency at a fixed magnetic field strength is further affected by unpaired spin density at the Fermi edge (Knight shift), thereby furnishing important information about the electronic band structure of the material.

However, severe limitations of solid-state NMR spectroscopy arise in the structural characterization of intermetallic compounds containing the rare-earth metals, because the localized paramagnetism of the incompletely occupied 4*f* shells results in ultrashort lifetimes of the nuclear Zeeman states thereby rendering signal observation impossible. This complication occurs in particular for the characterization of the local rare-earth environments themselves, which is possible only for the closed shell atomic configurations Sc^{3+}, Y^{3+}, La^{3+}, Yb^{2+} and Lu^{3+}. Among the corresponding nuclear isotopes listed in Table 1 only ^{45}Sc and ^{89}Y have been widely applied for the characterization of intermetallic and semiconducting compounds [4-9]. Ytterbium NMR spectroscopy in metallic compounds is limited to the relatively rare cases of divalent atomic cores [10], whereas the applicability of the lanthanum and lutetium isotopes is severely restricted by the large nuclear electric quadrupole moments

of the latter, producing tremendous spectral dispersion over a wide frequency range. As discussed in a recent review article about “exotic” nuclei [11], such quadrupolar interactions pose the principal impediment for structural solid state NMR studies. The ^{175}Lu and ^{176}Lu isotopes may well be considered the most “exotic” ones as they possess the largest nuclear electric quadrupole moments known in the group of stable isotopes [12]. As a consequence, very few NMR spectroscopic studies have been reported, all of which utilize the much more highly abundant ^{175}Lu isotope. The majority of these previous works are either nuclear quadrupole resonance studies carried out in the absence of Zeeman interactions [13-21], or they are wide-line NMR spectroscopic studies, probing the distribution of the local magnetic fields at the lutetium sites in cooperatively ordered magnetic materials over a frequency range of many MHz [22-29]. Classical static wide-line NMR spectroscopy has been applied to detect the ^{175}Lu NMR signal in LuAs [30], LuSb [31], LuB_{12} [31] and LuPtSb [32], but no significant information was obtained from those studies beyond the mere detection of the signal. The goal of the present study is to examine the feasibility of high-resolution ^{175}Lu NMR spectroscopy in cubic compounds and to characterize the internal interactions influencing those signals. The compounds chosen include the lutetium pnictides Lu*Pn* (NaCl-type structure; *Pn* = P, As, Sb), Lu*TX* compounds of the MgAgAs structure type (*T* = transition metal, *X* = group 13-15 element, see Figure 1), the Heusler phases LuT_2In (*T* = Cu, Au) as well as $LuPd_2Sn$. We present here the very first magic-angle spinning NMR spectroscopic data of the ^{175}Lu isotope.

Table 1: Available Nuclear Isotopes for NMR Studies of Rare-Earth Nuclei

Isotope	**Spin**	**Nat. abund.**	**γ (10^7 rad^{2}s^{-2})**	**eQ (10^{-28} m^2)**
^{45}Sc	7/2	100%	6.509	-0.22
^{89}Y	1/2	100%	-1.316	0
^{138}La	5	0.09%	3.557	0.45
^{139}La	7/2	99.91%	3.808	0.20
^{171}Yb	1/2	14.3%	4.729	0
^{173}Yb	5/2	16.4%	-1.303	2.8
^{175}Lu	7/2	97.4%	3.055	3.49
^{176}Lu	7	2.6%	2.168	4.97

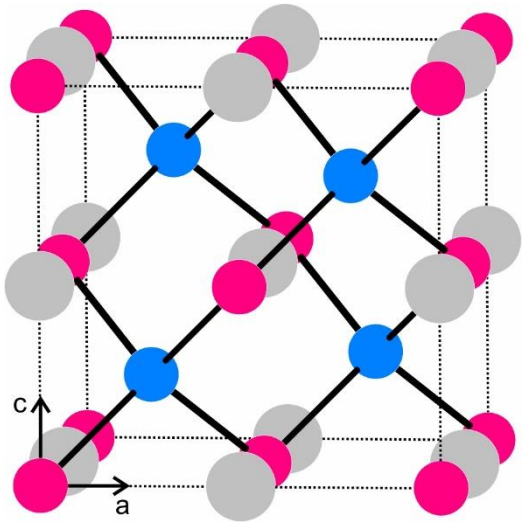

Fig. 1. The crystal structures of the cubic "half-Heusler" phases LuAuSn [36] and LuPtSb [37], crystallizing with the MgAgAs-type structure typical for some intermetallic compounds with the general composition *RETX* (*RE* = rare-earth metal, gray circles; *T* = transition metal, blue circles; *X* = group 13-15 element, magenta circles [38]). The lutetium atoms are tetrahedrally coordinated by the transition metal (Lu–*T* distances 284.3 and 279.6 pm) and by six Sn (Sb) atoms at distances of 328.3 and 322.8 pm, respectively.

2. Experimental

Sample preparation and characterization. Starting materials for the synthesis of the binary pnictides and the ternary lutetium compounds were dendritic pieces of lutetium (smart elements, 99.999%), red phosphorus (ABCR, 99.999%), arsenic pieces (Kelpin, 99.9%), antimony shots (VWR Int., 99.9%), nickel rods (Alfa Aesar, 99.5%), copper granules (Chempur, 99.999%), palladium and platinum sheets (Agosi, 99.9%), gold drops (Agosi, 99.9%), indium pieces (smart elements, 99.99%) and tin granules (Merck, p.a.). Several of the elements were additionally cleaned prior to the reactions: (i) the phosphorus pieces were cleaned with acetone and carefully crushed in a steel mortar under dry cyclohexane; (ii) the arsenic was resublimed twice in a sealed quartz tube to remove oxidic impurities; and (iii) the copper granules were treated shortly with hot concentrated hydrochloric acid followed by several washing steps with deionized water and finally ethanol.

Synthesis of LuP. Lutetium filings and phosphorus pieces were mixed under *cyclo*-hexane in the ideal atomic ratio of Lu:P = 1:1 (approx. 500 mg) and the dry powders were subsequently cold-pressed to a pellet of 6 mm diameter. The pellet was placed in an alumina crucible and sealed in an evacuated silica tube. The sample was heated at a rate of 30 K h^{-1} to 673 K in a muffle furnace and the temperature was kept for 24 h followed by a temperature increase at a rate of 40 K h^{-1} to 1223 K. After 7 days at that temperature, the ampule was quenched on a sand bath. In order to increase the homogeneity of the sample, the pellet was ground to a fine powder, re-pressed to a pellet and re-annealed at 1223 K for 12 h. This procedure was repeated three times and led to black LuP powder. As the compound has limited stability in air it is kept in the glove box over mineral oil for long term storage.

Synthesis of LuAs and LuSb. Around 600 mg of molar 1:1 ratios were arc-welded [33] in tantalum tubes and the elements were reacted by inductive heating in a water-cooled sample chamber [34] of a Hüttinger TIG 2.5/300 high-frequency furnace. The Ta containers were then sealed in evacuated silica ampules and annealed at 1223 K for 7 days. The annealing procedures led to grayish crystal agglomerates of LuAs and LuSb. The three pnictides are sensitive to air moisture and were kept under argon in Schlenk tubes prior to further use. The purity of the samples was checked through their Guinier powder pattern. The

refined lattice parameters of 553.35(6) pm for LuP, 567.9(1) pm for LuAs and 605.8(2) pm for LuSb are in excellent agreement with the literature data [35].

Synthesis of ternary Lu intermetallics. The ternary compounds with the nominal composition LuAuSn, Lu*T*Sb (*T* = Ni, Pd), LuT_2In (*T* = Cu, Au), and LuPd$_2$Sn were prepared by arc-melting [33] ideal-stoichiometric amounts of the elements in a water-cooled copper-hearth under an argon atmosphere of about 800 mbar. The argon gas was purified using titanium sponge (873 K), molecular sieves and silica gel. The as-prepared samples were subsequently enclosed in evacuated quartz tubes and were annealed for 10 d at 1073 K (LuAuSn and Lu*T*Sb) and 873 K (LuT_2In and LuPd$_2$Sn) in a tube furnace, respectively. The weight loss during preparation was less than 0.5%. Independent batches of LuAuSn and LuPtSb were prepared by arc-welding the elements into niobium ampules. The containers were subsequently placed in the water-cooled sample chamber of a high-frequency furnace (Hüttinger Elektronik, Freiburg Germany, Typ TIG 2.5/300) [34] and heated at 1473 K (10 min) and 1673 K (5 min), respectively, under a steady flow of argon, followed by shutting off the power supply. The temperature was controlled using an infra-red pyrometer (SensorTherm, Methis MS09) with a stated accuracy of ±50 K. Afterwards, the ampules were enclosed in evacuated quartz tubes and annealed at 1073 K for 10 d in a tube furnace. No reactions with the container material were observed for both compounds. All samples showed metallic luster, are stable in air over several months and are gray in their powdered forms.

Solid-State NMR spectroscopy. Solid-state NMR spectra were measured on Bruker DSX 400 and Avance Neo 600 spectrometers (^{175}Lu resonance frequencies of 45.27 and 67.96 MHz). At the magnetic flux density of 9.4 T, samples were rotated at MAS-frequencies between 11.0 and 12.0 kHz in 4mm rotors, while for the experiments at 14.1 T variable spinning speed measurements were done in 2.5 and 1.3 mm rotors, operated at MAS frequencies between 15.0 and 30.0 kHz. To facilitate spinning, minimize probe detuning and frictional heating effects of these metallic samples, finely ground mixtures containing 50 v/v KBr were measured. Measurement conditions are summarized in Table 2. The pulse lengths listed there are approximately half of those determined experimentally to yield the maximum signal on LuAuSn. This precaution was taken to ensure sufficiently small flip angles. Owing to very efficient quadrupolar relaxation, recycle delays of 0.20 to 0.5 s were found to be

sufficient for quantitative detection. In the case of the Heusler phases (only examined at 67.96 MHz) which gave no signals under these conditions, relaxation delays up to 10 s (10000 scans) were tried as well. Rolling baseline artifacts visible in the single-pulse spectra were removed by spline fitting. While identical spectra without baseline artifacts could be obtained using rotor-synchronized Hahn spin echo acquisition (4 rotor cycles), the signal-to-noise ratios were found to be significantly reduced, indicating either short spin-spin relaxation times and/or ill-defined π pulse lengths for these quadrupolar nuclei. For LuSb, LuPtSb and LuAuSn line broadening mechanisms were examined by field-dependent measurements at 14.1, 9.4, and 5.6 T, using single pulse detection. The measurements at 5.6 T were performed in an Agilent DD2 spectrometer in 1.6 mm rotors, 1.0 μs pulse length (selected following the criterion described above), 0.3 s recycle delay and ^{175}Lu resonance frequency of 24.39 MHz. Complementary characterizations of the other nuclear isotopes were also carried out. Single-pulse spectra were acquired at 9.4 T, at spinning frequencies between 10.0 and 12.0 kHz, using short pulses of 1.0 μs length for ^{75}As and ^{121}Sb, or 90° pulses of 5.0 μs length for the spin-1/2 nuclei ^{31}P and ^{195}Pt. Relaxation delays were between 0.5 and 2.0 seconds (20000-50000 scans).

Table 2 – Experimental parameters used to measure the single-pulse ^{175}Lu NMR spectra at magnetic field strengths of 9.4 and 14.1 T.

Sample	14.1 T			9.4 T		
	ν_R (kHz)	Pulse length (μs)	Recycle delay (s)	ν_R (kHz)	Pulse length (μs)	Recycle delay (s)
LuP	15.0	1.0	0.5	12.0	1.4	0.2
LuAs	25.0	1.0	0.4	11.0	1.4	0.2
LuSb	22.0	1.0	0.4	11.3	1.4	0.2
LuPtSb	30.0	1.0	0.3	11.5	1.4	0.2
LuAuSn	30.0	1.0	0.5	11.5	1.4	0.2

3. Results and Discussion

Figure 2 summarizes the ^{175}Lu NMR spectra of LuP, LuAs, LuSb, LuPtSb, and LuAuSn measured at 14.1 T. Although the spectra show many common features (as discussed below) there are large variations in the absolute signal intensity. This can be explained on the basis of structural defects, which produce electric field gradients (EFGs) at the nominally cubic Wyckoff sites occupied by the ^{175}Lu nuclei. As the magnitude of the EFG depends on the distance of the defect from the probe nucleus, a random distribution of defects will produce a distribution of EFGs. Given the large size of the ^{175}Lu nuclear electric quadrupole moment, the signal may be broadened beyond detectability by these EFGs if the defects are too close, and in compounds with high defect densities this can lead to complete signal obliteration. No ^{175}Lu NMR signals were observable in LuNiSb, $LuCu_2In$, $LuAu_2In$, and $LuPd_2Sn$ within the present study, even when exploring a wide range of measurement conditions. We attribute the failure of signal observation to these compounds to high defect densities.

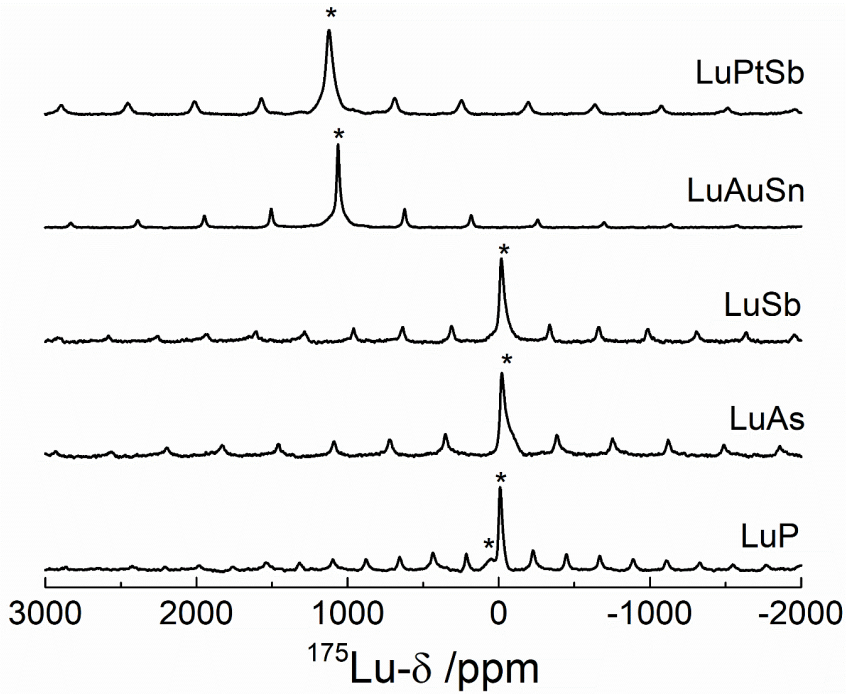

Figure 2: 14.1 T MAS-NMR spectra for some cubic Lu compounds. Central peaks are labelled by asterisks, and minor peaks are spinning sidebands.

Returning to Figure 2, by far the strongest signals were observed for the compounds LuP and LuAuSn. In both cases a signal-to-noise ratio sufficient for referencing can already be obtained within a few minutes, and noise-free spectra are available within 2 hours. In keeping with the tradition of choosing diamagnetic, non-metallic compounds as reference standards, we propose the compound LuP as the zero ppm standard; its exact resonance frequency at a magnetic flux density corresponding to 100.00 MHz proton frequency is given by 11.324 MHz.

The spectra displayed in Figure 2 reveal various features that can be seen as a common signature of ^{175}Lu NMR spectra in cubic compounds. In all cases, a relatively sharp central peak is seen, which arises from the $m = 1/2 \leftrightarrow m = -1/2$ transitions of the spin-7/2 isotope. This central signal is flanked by spinning sideband manifolds, arising from the anisotropically shifted non-central Zeeman ("satellite") transitions of those ^{175}Lu nuclei experiencing relatively weak electric field gradients produced by distant defects. This phenomenon has been previously discussed in the literature for numerous quadrupolar nuclei in cubic semiconductors [39, 40]. Under MAS conditions, these satellite transitions lead to the featureless spinning sideband patterns observed in Figure 2.

The dominant central ^{175}Lu resonances are characterized by isotropic shifts that clearly differentiate between the individual compounds. In the case of LuP, the main resonance is accompanied by one minor signal, which we attribute to either an impurity or a defect site with cubic symmetry. The peak positions and linewidths are independent of magnetic strength indicating the absence of second-order quadrupolar effects for these signals. The resonance frequencies of the lutetium pnictides are dominated by chemical shifts ($\delta_{iso} \sim$ -20 ppm vs. LuP), while those of LuAuSn and LuSbPt are affected by strong Knight shifts ($\delta_{iso} >$ 1000 ppm vs. LuP). In most of the cases the MAS-NMR linewidths are found independent of spinning frequencies (over the range of 11.0 to 30.0 kHz) within experimental error. An interesting exception occurs in the case of LuSb, which shows a broader central MAS-NMR linewidth at higher spinning frequencies (2.3 kHz at ν_R = 22.0 kHz versus 1.9 kHz at ν_R = 15.0 kHz). In addition, many spectra recorded at higher spinning speeds reveal broader signal components near the base of the peak, suggesting the detection of ^{175}Lu nuclei affected by stronger quadrupolar interactions.

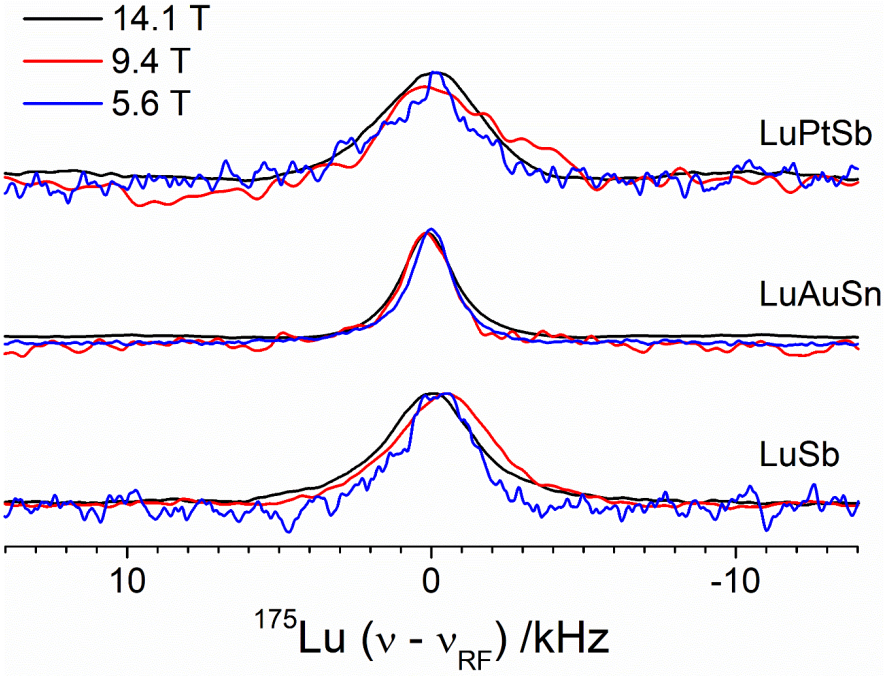

Figure 3: Static ^{175}Lu NMR spectra of LuSb, LuAuSn, and LuPtSb at different magnetic field strengths.

Note that despite the application of very fast MAS rotation speeds the NMR linewidths of the dominant signal components are still several kHz broad. To clarify the nature of the linebroadening mechanism, the static NMR linewidths of LuSb, LuPtSb and LuAuSn were measured at 5.6, 9.4 and 14.1 T (see Figure 3). Within experimental error, these linewidths (in kHz) are found to be independent of magnetic flux density. Thus they are neither affected by second-order quadrupolar broadening (inverse quadratic field dependence expected) nor by chemical or Knight shift distributions or anisotropies (linear field strength dependence expected). The dominant source of line broadening mechanism in these compounds are the direct and indirect homo- and heteronuclear spin-spin interactions, consisting of (1) the classical van Vleck (through-space) dipole-dipole contributions [41] (both homo- and heteronuclear), (2) the indirect (electronically mediated) heteronuclear interactions between the ^{175}Lu nuclei and the heteronuclei ^{121}Sb, ^{195}Pt, and $^{117/119}$Sn (historically called pseudo-dipolar interaction) and the indirect homonuclear ^{175}Lu-^{175}Lu spin-spin interactions (historically called pseudo-exchange interaction) [42, 43]. Table 3 indicates that magic angle

spinning effects only a modest improvement in resolution for the present compounds. As MAS is only able to remove the (anisotropic) van Vleck contributions, but not the isotropic pseudo-exchange and pseudo-dipolar couplings, we conclude that the latter interactions are the dominant line-broadening mechanism. Similar results have been observed in the MAS-NMR spectra of III-V semiconductors involving heavier elements [44]. For the present set of compounds the smallest MAS NMR linewidth is observed in LuAuSn, for which the heteronuclear pseudo-dipolar interactions can be considered particularly weak owing to the small magnetic moment of the ^{197}Au isotope and the low natural abundances of the magnetic tin isotopes, ^{115}Sn, ^{117}Sn, and ^{119}Sn.

Table 3: ^{175}Lu NMR isotropic shifts δ_{ms} and full widths at half maximum Δ measured under static and MAS conditions at different magnetic field strengths.

Compound	δ_{iso}/ppm(±2)		Δ_{MAS}/kHz(±0.2)		$\Delta_{stat.}$/kHz (±0.5)		
	14.1 T	9.4 T	14.1 T	9.4 T	14.1 T	9.4 T	5.6 T
LuP	0[a]	0	1.9	2.0	n.d.	n.d.	n.d.
LuAs	-20[b]	n.d.	2.2	n.d.	3.8	n.d.	n.d.
LuSb	-17[c]	-13	2.3	2.9	3.4	3.7	2.7
LuPtSb	1123	1121	3.2	3.0	4.5	4.6	4.5
LuAuSn	1064	1062	1.4	1.5	2.2	2.0	1.7

[a]minor signal at 62 ppm [b]shoulder at -70 ppm, c shoulder at -79 ppm

Table 4: MAS-NMR chemical shift and linewidths at 9.4 T of the non-rare-earth nuclei in the compounds under study, measured at 9.4 T.

Compound	δ_{iso}/ppm(±2)	Δ_{MAS}/kHz (±0.1)
Lu^{31}P[a]	553	1.4
Lu^{75}As[b]	1123	1.2
Lu^{121}Sb[c]	1682	2.3
LuPt^{121}Sb[c]	1676	6.7
Lu^{195}PtSb[d]	-3795	24.6
LuAu^{119}Sn[e]	273	2.8 [36]

Zero ppm reference standards: [a]85% H_3PO_4, [b]$NaAsF_6$(s), [c]$KSbF_6$(s), [d]K_2PtCl_6(s),[e]$Sn(CH_3)_4$ (l)

Table 4 also includes the results of NMR investigations on the non-rare earth nuclei, measured at 9.4 T. Their resonance frequencies are dominated by Knight shifts as well; the ^{31}P resonance shift measured for LuP is close to the value (500 ± 100) ppm reported by Jones

from static NMR measurements [45]. The substantial MAS-NMR linewidths of the pnictogen resonances again suggest strong exchange interactions. In addition, the ^{75}As and ^{121}Sb MAS-NMR spectra of LuAs and LuSb show wide spinning sideband patterns, which again reflect the anisotropic quadrupolar splittings arising from structural defects [39,40]. The ^{121}Sb Knight shifts of LuSb and LuPtSb are comparable to those measured in the compounds Sc*T*Sb (*T* = Ni, Pd, Pt), which also crystallize in the MgAgAs structure [46].

4. Conclusions

The large quadrupole moment of the ^{175}Lu nucleus restricts observation of the NMR spectroscopic signal to close to perfectly ordered crystalline samples with cubic local environments. Even small electric field gradients produced by remote structural defects or by mixed site occupancies in nominally cubic materials (a quite common occurrence in intermetallic compounds) can result in the complete obliteration of the NMR signal. We attribute our failure to observe signals in the Heusler phases LuT_2In (*T* = Cu, Au) to such mixed site occupancy effects as observed in the closely related isostructural Y- and Sc-containing compounds [47-49]. Signal detection is facilitated in cubic samples with significant covalent bonding character, in which such mixed site occupancies are thermodynamically disfavored. Thus, we were able to detect and characterize the resonances in the binary pnictides LuP, LuAs and LuSb (NaCl-type structure) and in LuAuSn and LuPtSb (MgAgAs-type structure). Even so, the signal in LuNiSb, which also crystallizes in the MgAgAs lattice, was not observable. Other candidates adopting this structure include LuPdSb and Lu*T*Bi (*T* = Ni, Pd, Pt). The preparation and characterization of high-quality samples in sufficient quantities for ^{175}Lu and ^{209}Bi NMR will be pursued in future studies.

An important conclusion of the present study is further, that the signal intensity and lineshape can vary significantly between different preparations, if these syntheses result in different concentrations and/or types of the residual defects. As these defects may generate a wide distribution of electric field gradients, the MAS-NMR linewidths may become spinning speed dependent, as noted for LuSb in the present work. Finally, the line narrowing achievable by MAS in intermetallic and semiconducting Lu compound is found to be

somewhat limited by the fact that the static NMR linewidths of this heavy element are dominated by isotropic pseudo-exchange and pseudo-dipolar interactions, which are not averaged out by MAS. The situation is expected to be different in cubic compounds with more ionic bonding character. The investigation of such crystalline materials is underway in our laboratories.

5. Acknowledgements

Funding by the DFG and by FAPESP (grants no 2013-07793-6 and 2013/23490-3) is most gratefully acknowledged.

6. References

[1] G. W. West, Philos. Mag. 8 (1964) 979.

[2] F. Haarmann, K. Koch, P. Jeglič, O. Pecher, H. Rosner, Yu. Grin, Chem. Eur. J. 17 (2011) 7560.

[3] C. Benndorf, H. Eckert, O. Janka, Acc. Chem. Res. 50 (2017) 1459.

[4] H. Eckert, R. Pöttgen, Z. Anorg. Allg. Chem. 636 (2010) 2232.

[5] L. Schubert, C. Doerenkamp, S. Haverkamp, L. Heletta, H. Eckert, R. Pöttgen, Dalton Trans. 47 (2018) 13025.

[6] T. Harmening, H. Eckert, C. M. Fehse, C. P. Sebastian, R. Pöttgen, J. Solid State Chem. 184 (2011) 3303.

[7] C. Höting, H. Eckert, F. Haarmann, F. Winter, R. Pöttgen, Dalton Trans. 43 (2014) 7860.

[8] C. P. Sebastian, L. Zhang, C. Fehse, R.-D. Hoffmann, H. Eckert, R. Pöttgen, Inorg. Chem. 46 (2007) 771.

[9] C. Höting, H. Eckert, S. F. Matar, U. Ch. Rodewald, R. Pöttgen, Z. Naturforsch. 69b (2014) 305.

[10] A. C. Gossard, V. Jaccarino, J. H. Wernick, Phys. Rev. 133 (1964) A881.

[11] C. Leroy, D. L. Bryce, Prog. Nucl. Magn. Reson. Spectrosc. 109 (2018) 160.

[12] N. J. Stone, J. Phys. Chem. Reference Data 44 (2015) 031215.

[13] K. B. Dillon, Spectrosc. Prop. Inorg. Organomet. Compd. 39 (2007) 187.

[14] A. G. Beda, A. A. Bush, A. F. Volkov, V. F. Meshcheryakov, Crystallogr. Rep. 50 (2005) 974.

[15] M. Yu. Burtsev, E. A. Kravchenko, A. G. Matyushkov, Zh. Fiz. Khim. 69 (1995) 1035.

[16] M. Yu. Burtsev, A. V. Tararov, A. G. Dudareva, E. A. Kravchenko, Zh. Neorg. Khim. 39 (1994) 306.

[17] P.-J. Chu, B. C. Gerstein, H. D. Yang, R. N. Shelton, Phys. Rev. B 37 (1988) 1796.

[18] V. A. Vasilkovskii, A. A. Gorlenko, V. F. Ostrovskii, Fiz. Tverd. Tela 34 (1992) 2103.

[19] G. K. Semin, A. M. Raevskii, JETP 44 (1986) 461.

[20] A. F. Volkov, Zh. Fiz. Khim. 54 (1980) 3058.

[21] A. F. Volkov, A. A. Ivanova, Yu. N. Venevtseve, L. L. Rapoport, Zh. Fiz. Khim 56 (1982) 1002.

[22] J. Schnelzer, R. Montbrun, B. Pilawa, G. Fischer, G. Venturini, E. Dormann, Eur. Phys. J. B 58 (2007) 11.

[23] K. Shimizu, F. Ogarawawara, K. Ichinose, Physica B 237-238 (1997) 584.

[24] Y. Kasamatsu, J. G. M. Armitage, J. S. Lord, P. C. Riedi, D. Fort, J. Magn. Magn. Mater. 140-144 (1995) 819.

[25] K. Shimizu, J. Magn. Magn. Mater. 70 (1987) 178.

[26] K. Shimizu, N. Sano, J. Itoh, J. Phys. Soc. Jpn. 39 (1975) 539.

[27] D. M. Eagles, P. Lalousis, Hyperfine Interact. 8 (1980) 283.

[28] L. Dang Khoi, M. Rotter, Phys. Lett. A 34 (1971) 382.

[29] R. Gonano, E. Hunt, H. Meyer, Phys. Rev. 156 (1967) 521.

[30] O. Żogal, R. Wawryk, M. Matusiak, Z. Henkie, J. Alloys Compd. 587 (2014) 190.

[31] A. H. Reddoch, G. J. Ritter, Phys. Rev. 126 (1962) 1493.

[32] B. Nowak, D. Kaczorowski, Intermetallics 40 (2013) 28.

[33] R. Pöttgen, T. Gulden, A. Simon, GIT Labor-Fachzeitschrift 43 (1999) 133.

[34] R. Pöttgen, A. Lang, R.-D. Hoffmann, B. Künnen, G. Kotzyba, R. Müllmann, B. D. Mosel, C. Rosenhahn, Z. Kristallogr. 214 (1999) 143.

[35] A. Iandelli, G. B. Bonino, Atti Accad. Naz. Lincei, Cl. Sci. Fis., Mat. Nat., Rend. 37 (1964) 160.

[36] C. P. Sebastian, H. Eckert, S. Rayaprol, R.-D. Hoffmann, R. Pöttgen, Solid State Sci. 8 (2006) 560.

[37] A. E. Dwight, Proc. Rare Earth Res. Conf. 11th 2 (1974) 642.

[38] H. Nowotny, W. Sibert, Z. Metallkd. 33 (1941) 391.

[39] R. G. Shulman, B. J. Wyluda, P. W. Anderson, Phys. Rev. 107 (1957) 953.

[40] R. K. Sundfors, Phys. Rev. 185 (1969) 458.

[41] J. H. van Vleck, Phys. Rev. 54, (1948), 1168

[42] M. A. Ruderman and C. Kittel, Phys. Rev. 96 (1954), 99

[43] N. Bloembergen, T. J. Rowland, Phys. Rev. 97 (1955), 1679.

[44] O. H. Han, H. K. C. Timken, E. Oldfield, J. Chem. Phys. 80 (1988) 6046.

[45] E. D. Jones, Phys. Rev. 180 (1969) 455

[46] T. Harmening, H. Eckert, R. Pöttgen, Solid State Sci. 11 (2009) 900.

[46] T. Graf, C. Felser, S.S. P. Parkin, Progr. Solid State Chem. 39 (2011) 1.

[47] C. Benndorf, S. Stein, L. Heletta, M. Kersting, H. Eckert, R. Pöttgen, Dalton Trans. 46 (2017) 250.

[48] M. Johnscher, S. Stein, O. Niehaus, C. Benndorf, L. Heletta, M. Kersting, C. Höting, H. Eckert, R. Pöttgen, Solid State Sci. 52 (2015) 57.

[49] C. Benndorf, O. Niehaus, H. Eckert, O. Janka, Z. Anorg. Allg. Chem. 641 (2015) 168.